Matthews, J.J., Liu, A.G., Yang, C., McIlroy, D., Levell, B., and Condon, D.J., 2020, A Chronostratigraphic Framework for the Rise of the Ediacaran Macrobiota: New Constraints from Mistaken Point Ecological Reserve, Newfoundland: GSA Bulletin, https://doi.org/10.1130/B35646.1.

Supplemental Material

SUPPLEMENTARY INFORMATION 1 (SI1): SAMPLED TUFFITES

SUPPLEMENTARY INFORMATION 2 (SI2): Information used in compiling macrofossil stratigraphic ranges

SUPPLEMENTARY INFORMATION 3 (SI3): U-Pb CA-ID-TIMS methods

SUPPLEMENTARY INFORMATION 4 (SI4): U-Pb Compositional and Isotopic Data

SUPPLEMENTARY INFORMATION 5 (SI5)

SUPPLEMENTARY INFORMATION 1 (SI1): SAMPLED TUFFITES

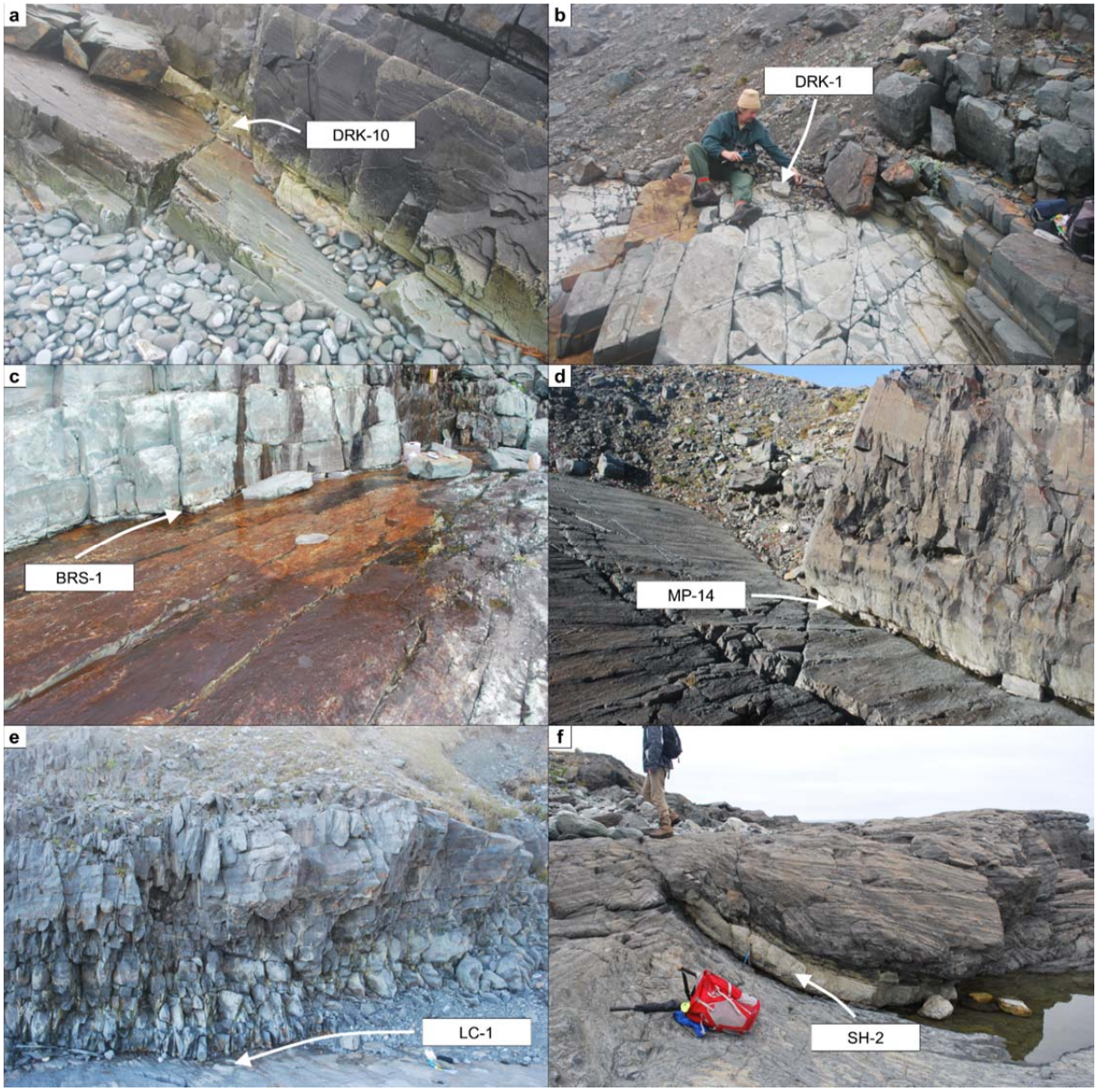

FIGURE S1. Field locality photographs for the sampled tuffites within MPER. **A:** DRK-10 above the Pizza Disc surface, Pigeon Cove, Drook Fm. **B:** DRK-1, near Drook, in the lower Briscal Fm. **C:** BRS-1, above the Brasier Surface in the Briscal Fm. **D:** MP-14 above the 'E' Surface, Mistaken Point, Mistaken Point Fm. **E:** LC-1 above the 'Pizzeria', Trepassey Fm. **F:** SH-2, Fermeuse Fm. at Shingle Head.

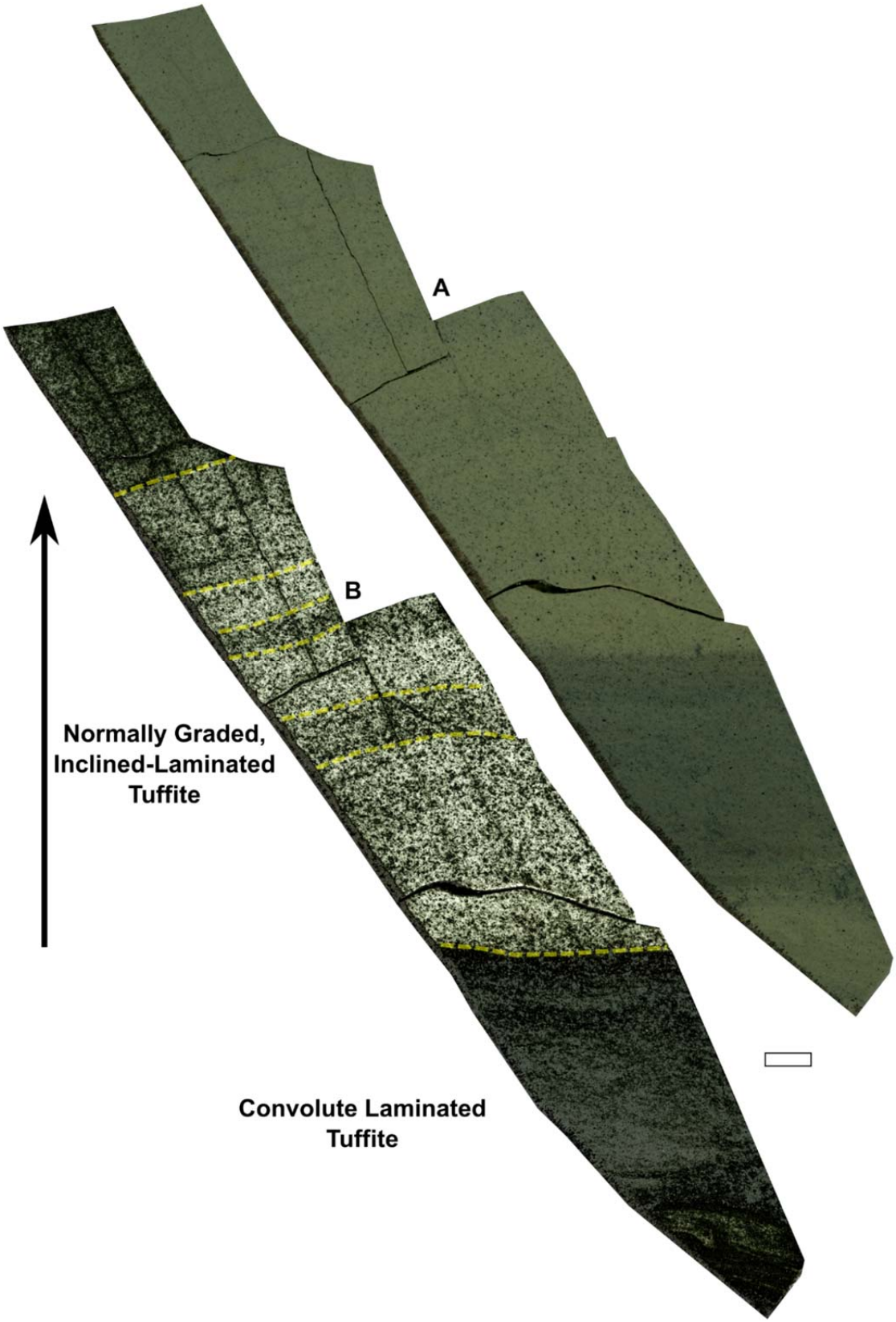

FIGURE S2. Slabbed and polished sample of the DRK-10 tuffite. **A:** True color scan. **B:** False color image to emphasize internal structures within the unit. Scale bar is 1 cm. Sample housed in the Oxford University Museum of Natural History, accession number AccSer.35281.

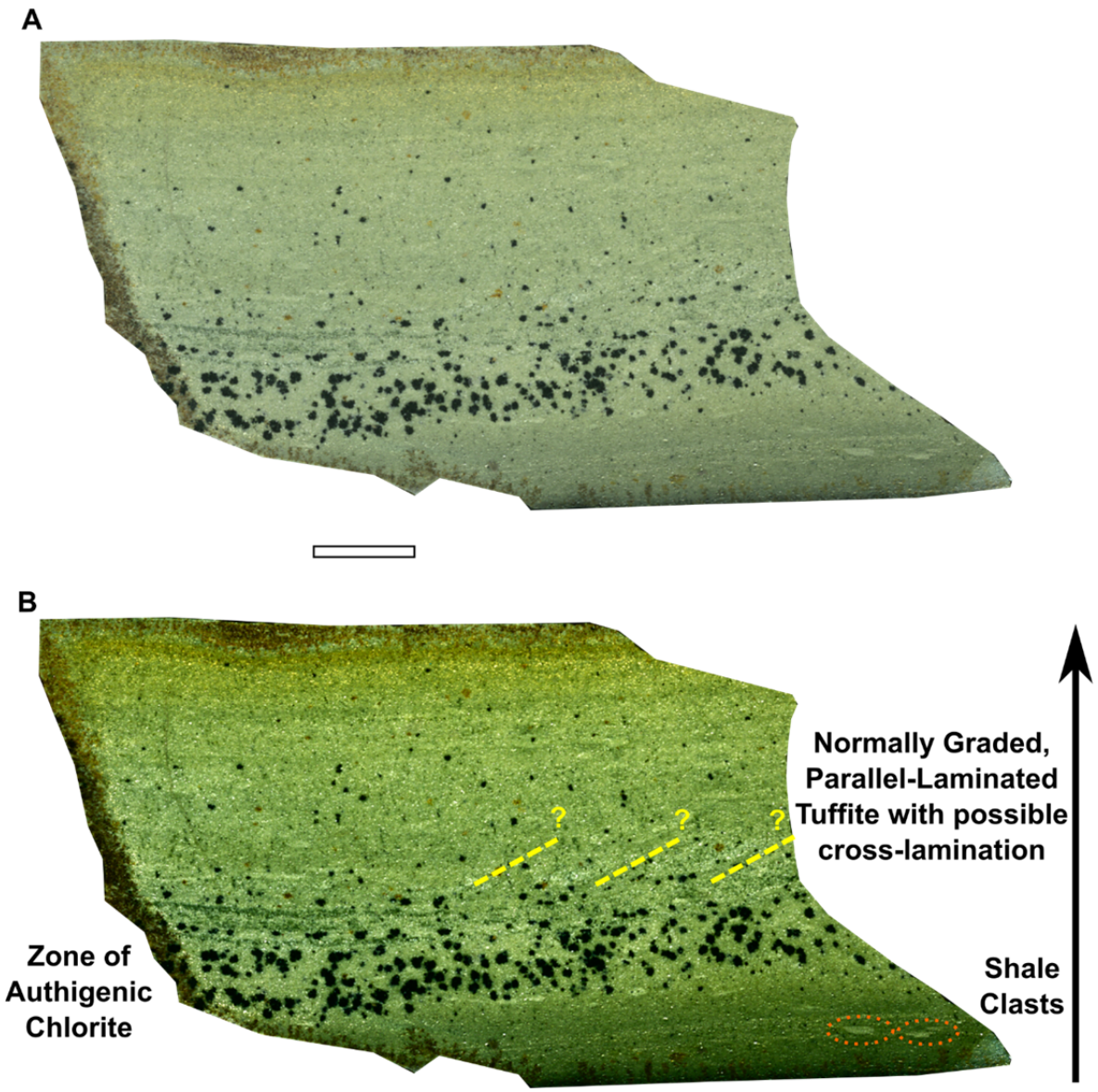

FIGURE S3. Slabbed and polished sample of the DRK-1 tuffite. **A:** True color scan. **B:** False color image to emphasize internal structures within the unit. Scale bar is 1 cm. Sample housed in the Oxford University Museum of Natural History, accession number AccSer.35282.

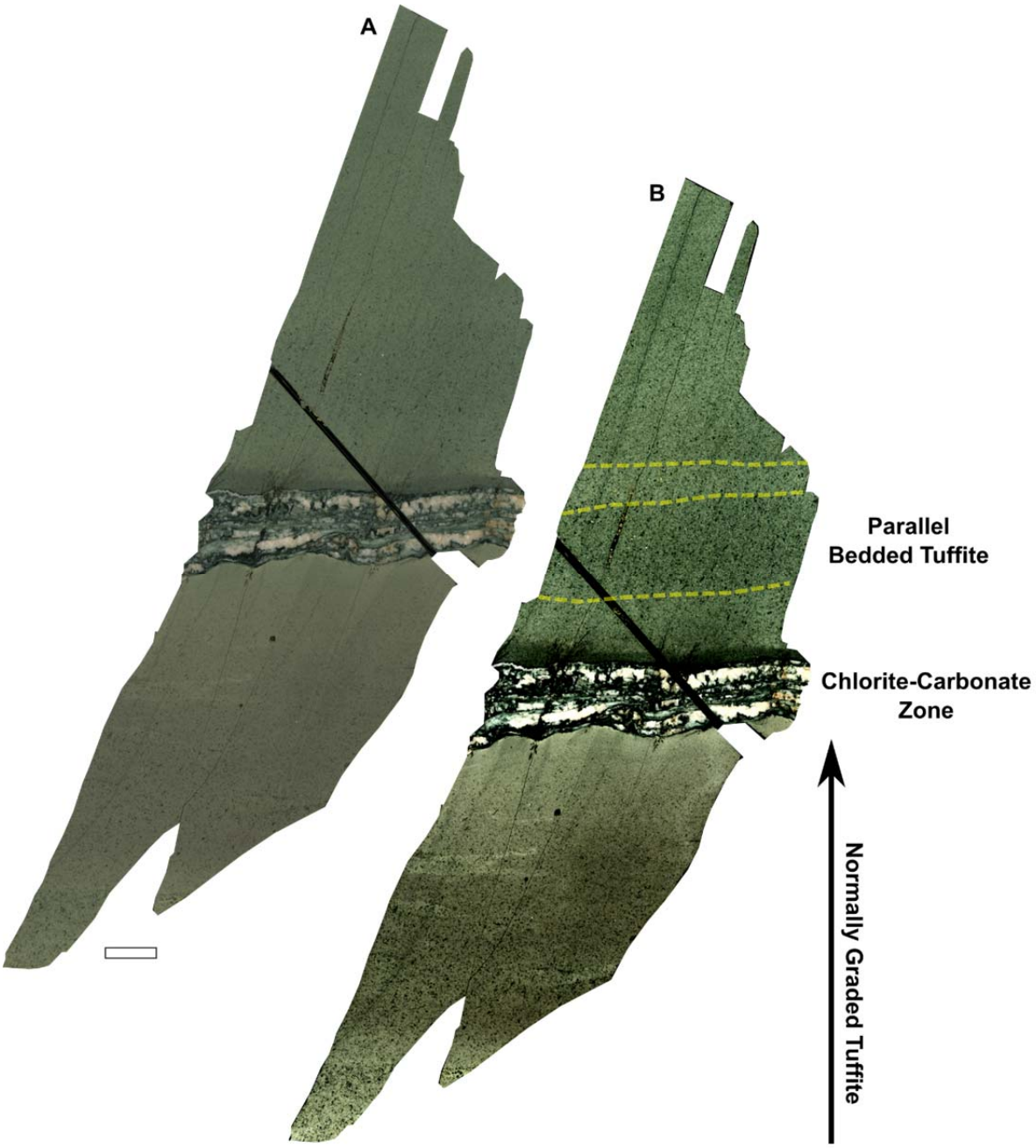

FIGURE S4. Slabbed and polished sample of the MP-14 tuffite. **A:** True color scan. **B:** False color image to emphasize internal structures within the unit. Scale bar is 1 cm. Sample housed in the Oxford University Museum of Natural History, accession number AccSer.35283.

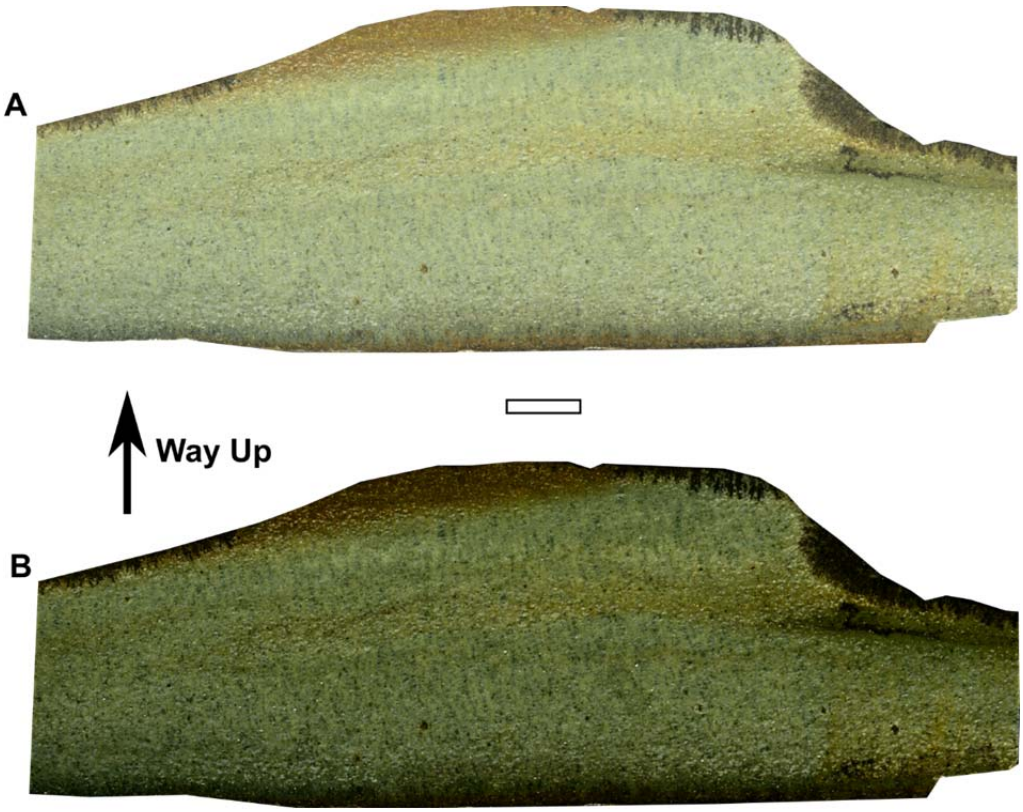

FIGURE S5. Slabbed and polished sample of the LC-1 tuffite. **A:** True color scan. **B:** False color image to emphasize internal structures within the unit. Scale bar is 1 cm. Sample housed in the Oxford University Museum of Natural History, accession number AccSer.35284.

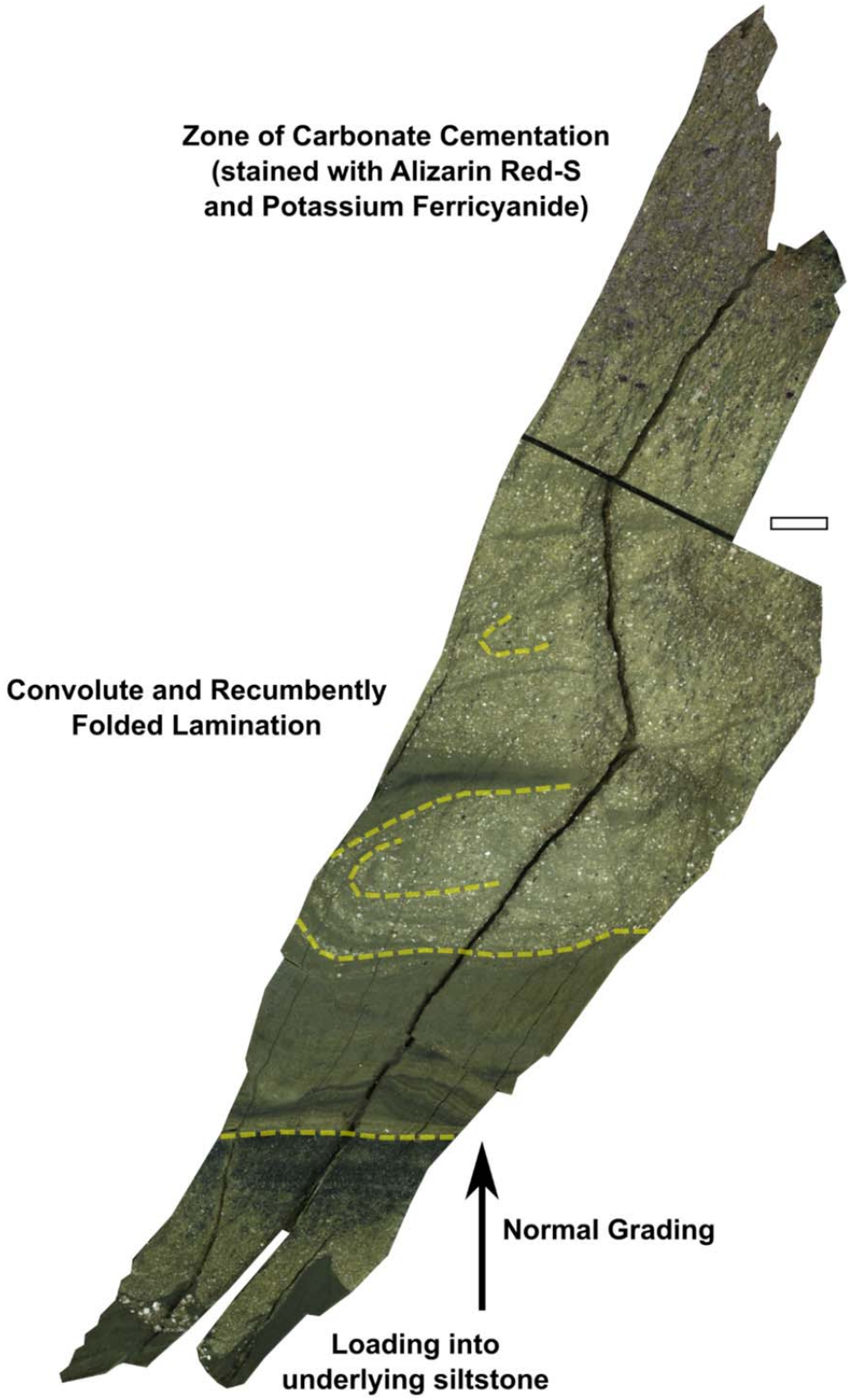

FIGURE S6. True color image of a slabbed and polished sample of the SH-2 tuffite. The top section of the slab has been stained for carbonate using Alizarin Red-S and Potassium Ferricyanide. Scale bar is 1 cm. Sample housed in the Oxford University Museum of Natural History, accession number AccSer.35285.

SUPPLEMENTARY INFORMATION 2 (SI2): Information used in compiling macrofossil stratigraphic ranges

The occurrence of fossils on bedding planes within MPER was documented over the course of multiple years by AGL. Field notes on the presence of individual taxa were cross-checked against photographic records of each surface, and only taxa that could be confidently identified were included in this study. Information regarding relative abundance of taxa on individual surfaces was not collected for all surfaces, and therefore is not included here. Since the weather and lighting conditions under which a surface is viewed can substantially impact an observer's ability to recognize fossils, we endeavored to search for specimens in the MPER at least twice over the period of study. However, we know that there are some previously documented levels at which we did not observe fossils, and so we acknowledge that this compilation is not 100% complete. Every effort was made to access and assess all available bedding plane surfaces where it was safe to do so, but certain sections of the stratigraphy (notably in the middle of the Mistaken Point Formation, and the upper Trepassey Formation) were too inaccessible or poorly exposed for data to be gathered.

Taxa were identified to species level wherever possible. Specimens of *Primocandelabrum* in Newfoundland have historically only been divided into *Primocandelabrum hiemaloranum* (showing a clear *Hiemalora*-type holdfast structure), and *Primocandelabrum* sp. This latter grouping could include specimens referred to *P. boyntoni*, *P. aethelflaedia*, and *P. aethelwynnia* from Charnwood Forest, UK (Kenchington and Wilby, 2017; though see also Mitchell et al., 2018), but since the Newfoundland taxa are yet to be subjected to detailed morphological analysis, we have not distinguished between those taxa in this study.

We recognized a number of undocumented taxa or ancilliary impressions occurring as rare components of the paleocommunities, but apart from filaments (see Liu and Dunn, 2020) and the 'string organism', we have not included these within the main figures. Lobate discs, previously noted as distinct impressions (Clapham et al., 2003), have been grouped with ivesheadiomorphs in this study, although we recognize that they may be discrete structures. Lobate discs were only identified at two horizons within MPER, on the 'E' and 'G' surfaces.

In addition to our primary field surveys, we also collated fossil occurrence data from the available literature (see the following list of publications). Data from publications were only included if we could be confident of the position of the studied horizon within our stratigraphic column, and if we were confident that the fossil would have been correctly identified. In some instances a paper mentions the presence of a taxon, but because we couldn't verify precisely which surface was being referred to, those occurrences have not been included (e.g., some *Charnia* and *Trepassia* in Narbonne and Gehling 2003; some *Vinlandia* and *Trepassia* in Laflamme et al., 2007; and some Ivesheadiomorphs in Laflamme et al., 2012). We were also unable to include data from several field guides in which fossil-bearing surfaces are documented, but assemblage composition is not presented (e.g., Narbonne et al., 2005). The presence of *Arborea arborea* within MPER follows synonymisation of *Charniodiscus arboreus* within that taxon by Laflamme et al. (2018).

References used in compiling the stratigraphic ranges, or cited in this section

Anderson, M.M., and Conway Morris, S., 1982, A review, with descriptions of four unusual forms, of the soft-bodied fauna of the Conception and St. John's Groups (Late Precambrian), Avalon Peninsula, Newfoundland: Proceedings of the third North American paleontological convention, v. 1, p. 1–8.

Bamforth, E.L., and Narbonne, G.M., 2009, New Ediacaran rangeomorphs from Mistaken Point, Newfoundland, Canada: Journal of Paleontology, v. 83, p. 897–913, https://doi.org/10.1666/09-047.1.

Bamforth, E.L., Narbonne, G.M., and Anderson, M.M., 2008, Growth and ecology of a multi-branched Ediacaran rangeomorph from the Mistaken Point assemblage, Newfoundland: Journal of Paleontology, v. 82, p. 763–777, https://doi.org/10.1666/07-112.1.

Brasier, M.D., and Antcliffe, J.B., 2009, Evolutionary relationships within the Avalonian Ediacara biota: new insights from laser analysis: Journal of the Geological Society, v. 166, p. 363–384, https://doi.org/10.1144/0016-76492008-011.

Brasier, M.D., Antcliffe, J.B., and Liu, A.G., 2012, The architecture of Ediacaran fronds: Palaeontology, v. 55, p. 1105–1124, https://doi.org/10.1111/j.1475-4983.2012.01164.x.

Clapham, M.E., Narbonne, G.M., and Gehling, J.G., 2003, Paleoecology of the oldest known animal communities: Ediacaran assemblages at Mistaken Point, Newfoundland: Paleobiology, v. 29, p. 527–544, https://doi.org/10.1666/0094-8373(2003)029<0527:POTOKA>2.0.CO;2.

Darroch, S.A., Laflamme, M., and Wagner, P.J., 2018, High ecological complexity in benthic Ediacaran communities: Nature Ecology & Evolution, v. 2, p. 1541–1547, https://doi.org/10.1038/s41559-018-0663-7.

Dunn, F.S., Wilby, P.R., Kenchington, C.G., Grazhdankin, D.V., Donoghue, P.C., and Liu, A.G., 2019, Anatomy of the Ediacaran rangeomorph *Charnia masoni*: Papers in Palaeontology, v. 5, p. 157–176, https://doi.org/10.1002/spp2.1234.

Flude, L.I., and Narbonne, G.M., 2008, Taphonomy and ontogeny of a multibranched Ediacaran fossil: *Bradgatia* from the Avalon Peninsula of Newfoundland: Canadian Journal of Earth Sciences, v. 45, p. 1095–1109, https://doi.org/10.1139/E08-057.

Gehling, J.G., and Narbonne, G.M., 2007, Spindle-shaped Ediacara fossils from the Mistaken Point assemblage, Avalon zone, Newfoundland: Canadian Journal of Earth Sciences, v. 44, p. 367–387, https://doi.org/10.1139/e07-003.

Hofmann, H.J., O'Brien, S.J., and King, A.F., 2008, Ediacaran biota on bonavista peninsula, Newfoundland, Canada: Journal of Paleontology, v. 82, p. 1–36, https://doi.org/10.1666/06-087.1.

Kenchington, C.G., and Wilby, P.R., 2017, Rangeomorph classification schemes and intra-specific variation: are all characters created equal?: Geological Society of London, Special Publications, v. 448, p. 221–250, https://doi.org/10.1144/SP448.19.

Laflamme, M., and Narbonne, G.M., 2008, Competition in a Precambrian world: palaeoecology of Ediacaran fronds: Geology Today, v. 24, p. 182–187, https://doi.org/10.1111/j.1365-2451.2008.00685.x.

Laflamme, M., Narbonne, G.M., and Anderson, M.M., 2004, Morphometric analysis of the Ediacaran frond *Charniodiscus* from the Mistaken Point Formation, Newfoundland: Journal of Paleontology, v. 78, p. 827–837, https://doi.org/10.1666/0022-3360(2004)078<0827:MAOTEF>2.0.CO;2.

Laflamme, M., Narbonne, G.M., Greentree, C., and Anderson, M.M., 2007, Morphology and taphonomy of an Ediacaran frond: *Charnia* from the Avalon Peninsula of Newfoundland:

Geological Society of London, Special Publications, v. 286, p. 237–257, https://doi.org/10.1144/SP286.17.
Laflamme, M., Flude, L.I., and Narbonne, G.M., 2012, Ecological tiering and the evolution of a stem: the oldest stemmed frond from the Ediacaran of Newfoundland, Canada: Journal of Paleontology, v. 86, p. 193–200, https://doi.org/10.1666/11-044.1.
Laflamme, M., Gehling, J.G., and Droser, M.L., 2018, Deconstructing an Ediacaran frond: three-dimensional preservation of *Arborea* from Ediacara, South Australia: Journal of Paleontology, v. 92, p. 323–335, https://doi.org/10.1017/jpa.2017.128.
Landing, E., Narbonne, G.M., Myrow, P., Benus, A.P., and Anderson, M.M., 1988, Faunas and depositional environments of the Upper Precambrian through Lower Cambrian, southeastern Newfoundland: Bulletin - New York State Museum, v. 463, p. 8–52.
Liu, A.G., and Matthews, J.J., 2017, Great Canadian Lagerstätten 6. Mistaken Point Ecological Reserve, Southeast Newfoundland: Geoscience Canada, v. 44, p. 63–76, https://doi.org/10.12789/geocanj.2017.44.117.
Liu, A.G., and Dunn, F.S., 2020, Filamentous connections between Ediacaran fronds: Current Biology, v. 30, p. 1322–1328, https://doi.org/10.1016/j.cub.2020.01.052.
Liu, A.G., McIlroy, D., and Brasier, M.D., 2010, First evidence for locomotion in the Ediacara biota from the 565 Ma Mistaken Point Formation, Newfoundland: Geology, v. 38, p. 123–126, https://doi.org/10.1130/G30368.1.
Liu, A.G., McIlroy, D., Antcliffe, J.B., and Brasier, M.D., 2011, Effaced preservation in the Ediacara biota and its implications for the early macrofossil record: Palaeontology, v. 54, p. 607–630, https://doi.org/10.1111/j.1475-4983.2010.01024.x.
Liu, A.G., McIlroy, D., Matthews, J.J., and Brasier, M.D., 2012, A new assemblage of juvenile Ediacaran fronds from the Drook Formation, Newfoundland: Journal of the Geological Society, v. 169, p. 395–403, https://doi.org/10.1144/0016-76492011-094.
Liu, A.G., Kenchington, C.G., and Mitchell, E.G., 2015, Remarkable insights into the paleoecology of the Avalonian Ediacaran macrobiota: Gondwana Research, v. 27, p. 1355–1380, https://doi.org/10.1016/j.gr.2014.11.002.
Mason, S.J., and Narbonne, G.M., 2016, Two new Ediacaran small fronds from Mistaken Point, Newfoundland: Journal of Paleontology, v. 90, p. 183–194, https://doi.org/10.1017/jpa.2016.14.
Matthews, J.J., Liu, A.G., and McIlroy, D., 2017, Post-fossilization processes and their implications for understanding Ediacaran macrofossil assemblages: Geological Society of London, Special Publications, v. 448, p. 251–269, https://doi.org/10.1144/SP448.20.
Mitchell, E.G., and Kenchington, C.G., 2018, The utility of height for the Ediacaran organisms of Mistaken Point: Nature Ecology & Evolution, v. 2, p. 1218–1222, https://doi.org/10.1038/s41559-018-0591-6.
Mitchell, E.G., Kenchington, C.G., Harris, S., and Wilby, P.R., 2018, Revealing rangeomorph species characters using spatial analyses: Canadian Journal of Earth Sciences, v. 55, p. 1262–1270, https://doi.org/10.1139/cjes-2018-0034.
Narbonne, G.M., and Gehling, J.G., 2003, Life after snowball: the oldest complex Ediacaran fossils: Geology, v. 31, p. 27–30, https://doi.org/10.1130/0091-7613(2003)031<0027:LASTOC>2.0.CO;2.
Narbonne, G.M., Dalrymple, R.W., Laflamme, M., Gehling, J.G., and Boyce, W.D., 2005, Life after snowball: Mistaken Point Biota and the Cambrian of the Avalon: North American paleontological convention field trip guidebook, 98 p.

Narbonne, G.M., Laflamme, M., Greentree, C., and Trusler, P., 2009, Reconstructing a lost world: Ediacaran rangeomorphs from Spaniard's Bay, Newfoundland: Journal of Paleontology, v. 83, p. 503–523, https://doi.org/10.1666/08-072R1.1.

SUPPLEMENTARY INFORMATION 3 (SI3): U-Pb CA-ID-TIMS methods

Zircons were separated from each sample using conventional mineral separation techniques. They were pretreated by a chemical abrasion technique after Mattinson (2005), which involved thermal annealing in a furnace at 900 °C for 60 h, followed by partial dissolution in 29M HF at 180 °C in high-pressure vessels for 12 h. The chemically abraded grains were fluxed in/rinsed with several hundred microliters of dilute HNO_3 and 6M HCl to remove the leachates.

All zircon fragments were spiked with the EARTHTIME ET535 (or ET2535) mixed ^{205}Pb-^{233}U-^{235}U ($\pm^{202}Pb$) isotopic tracer(s) (Condon et al. 2015; McLean et al. 2015) prior to complete dissolution in 29M HF at 220 °C for 60 h and subsequent Pb and U purification by an HCl-based anion-exchange column chemistry (Krogh, 1973). Pb and U were loaded together onto single outgassed Re filaments along with a silica-gel emitter solution and their isotopic ratios were measured on a Thermo-Electron Triton instrument equipped with an ion-counting SEM system. Pb was measured in dynamic mode on a MassCom secondary electron multiplier (SEM) and was corrected for mass bias using a fractionation factor of 0.14 ± 0.02%/amu (1σ) for samples prepared using the ET535 spike, and in real-time, based on measured $^{202}Pb/^{205}Pb$ ratios, for samples spiked with the ET2535 tracer. U isotopes were measured as dioxide ions either in static mode, on Faraday detectors equipped with 10^{12} Ω resistors for intensities greater than 4 mV, or in dynamic mode for lower intensities. U mass fractionation was calculated in real-time based on the isotopic composition of the ET535 and ET2535 tracers. Oxide correction was based on an $^{18}O/^{16}O$ ratio of 0.00205 ± 0.00004, and the sample $^{238}U/^{235}U$ ratio was assumed 137.818 ± 0.045 (Hiess et al., 2012).

Data reduction, calculation of dates and propagation of uncertainties used the Tripoli and ET_Redux applications and algorithms (McLean et al. 2011).

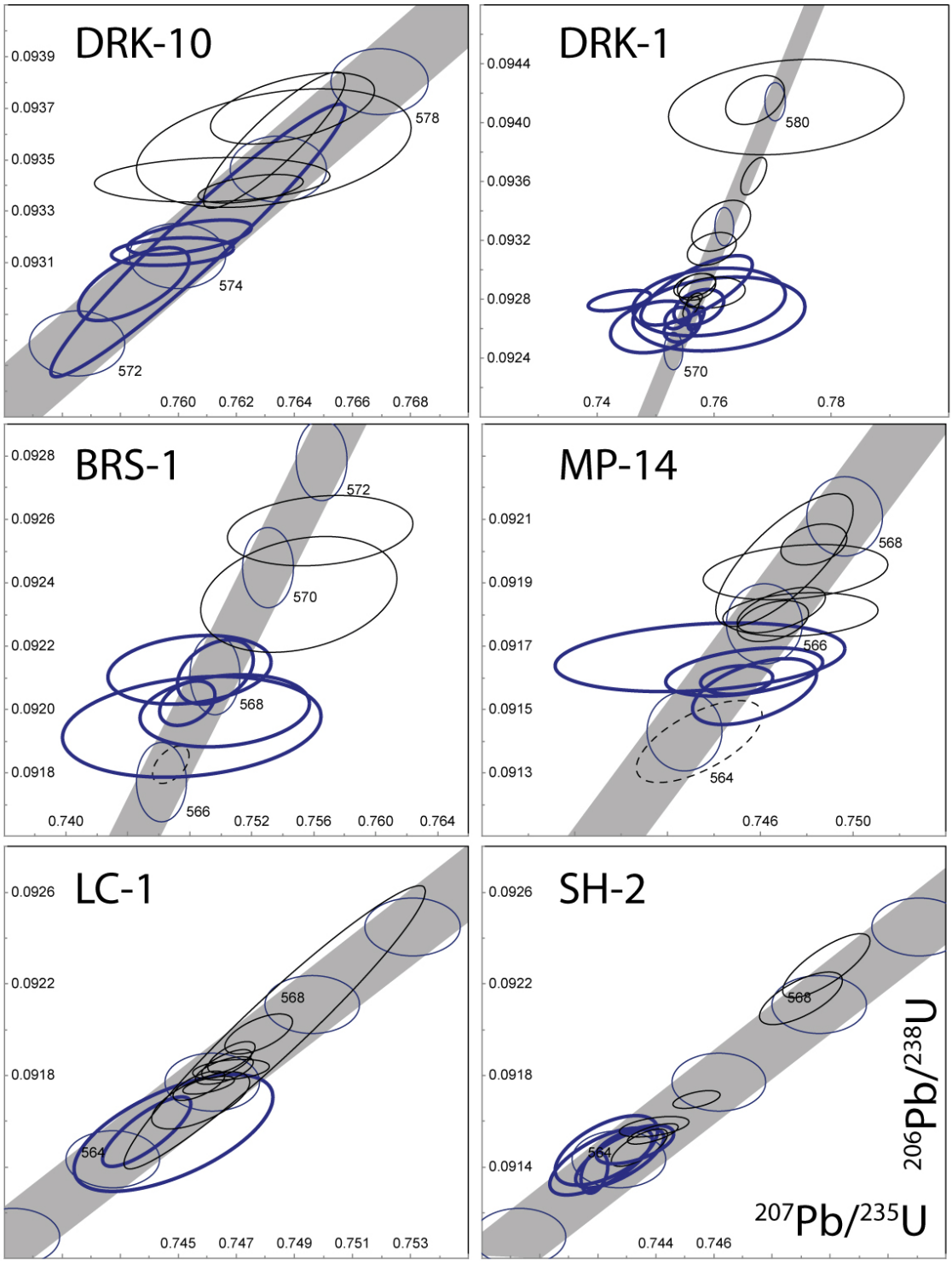

Figure S7. Conventional U-Pb concordia plots for the six samples analyzed in this study. Blue ellipses are those analyses used in the weighted mean calculations, dashed ellipses are interpreted as reflecting post-depositional Pb-loss, other older analyses reflect 'inheritance'.

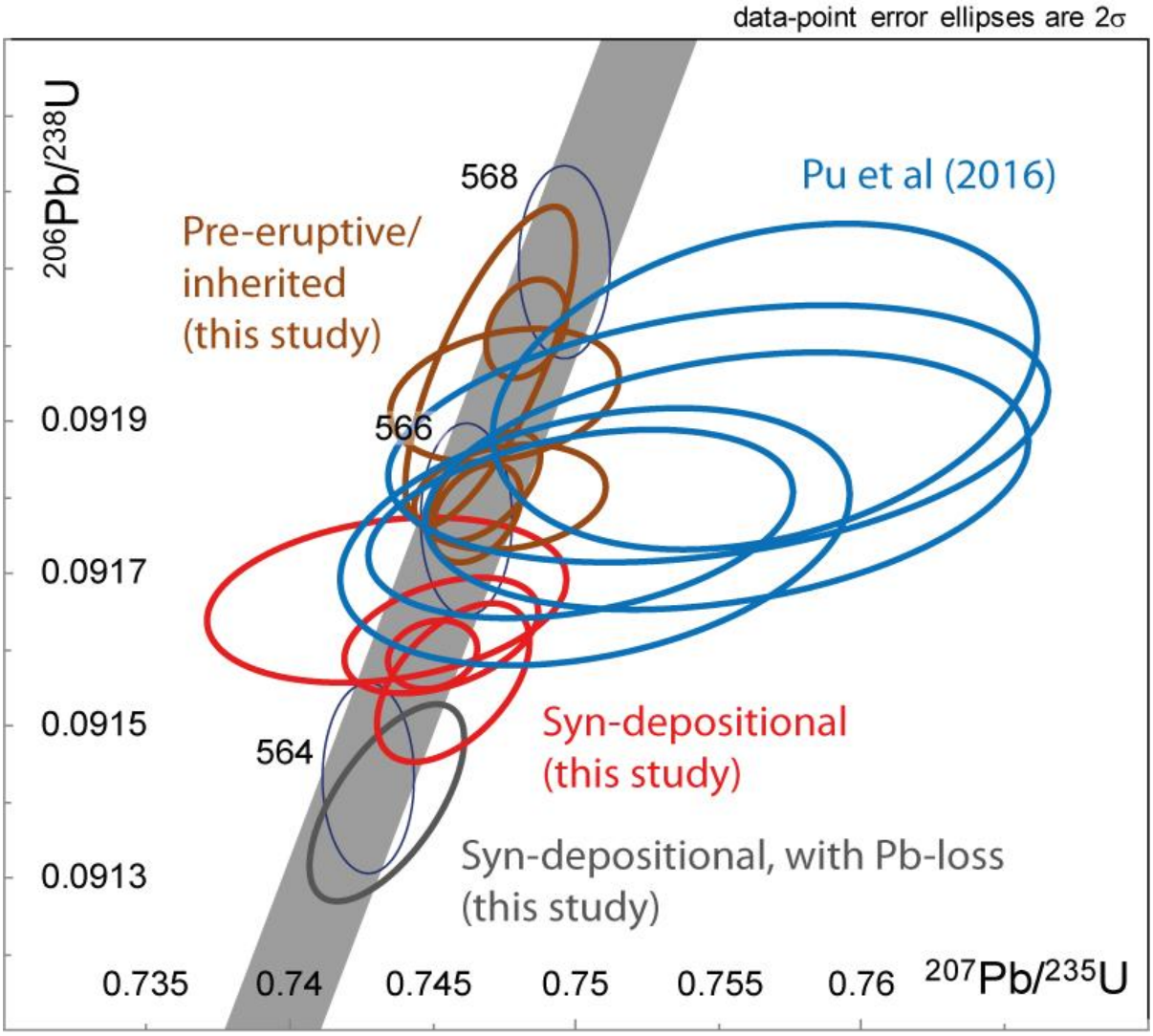

Figure S8. U-Pb Concordia plot for U-Pb (zircon) data from the 'E' Surface ash layer, sample MP-14 (this study) and sample MPMP33.56 (Pu et al., 2016).

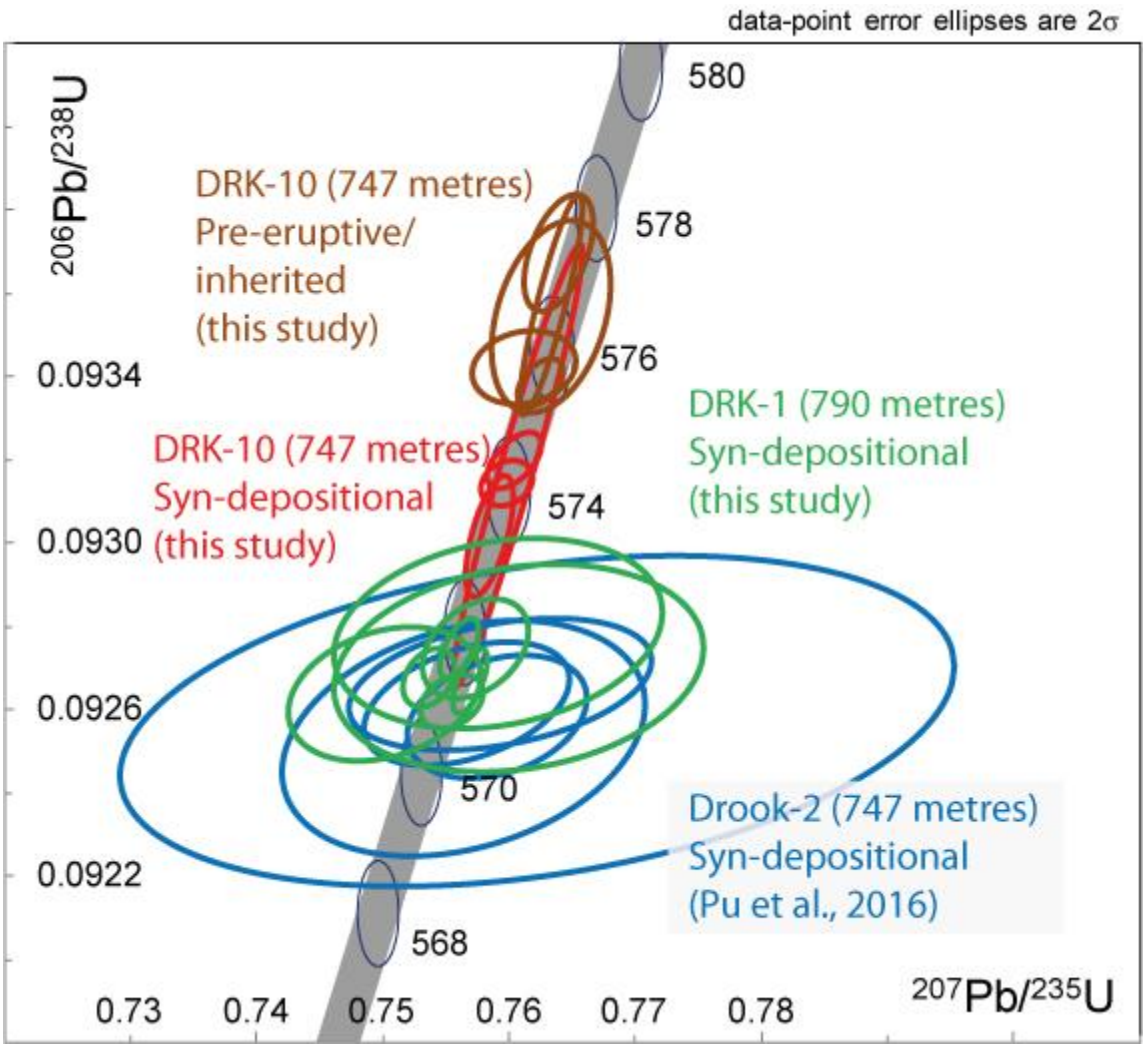

Figure S9. U-Pb Concordia plot for U-Pb (zircon) data from the 'Pizza Disc' ash layer, sample DRK-10 (this study) and sample Drook-2 (Pu et al., 2016). Also plotted is the U-Pb (zircon) data from sample DRK-1 (this study) that lies ~43 m up section of the 'Pizza Disc' ash layer which we interpret as being similar in age to the zircon from Drook-2.

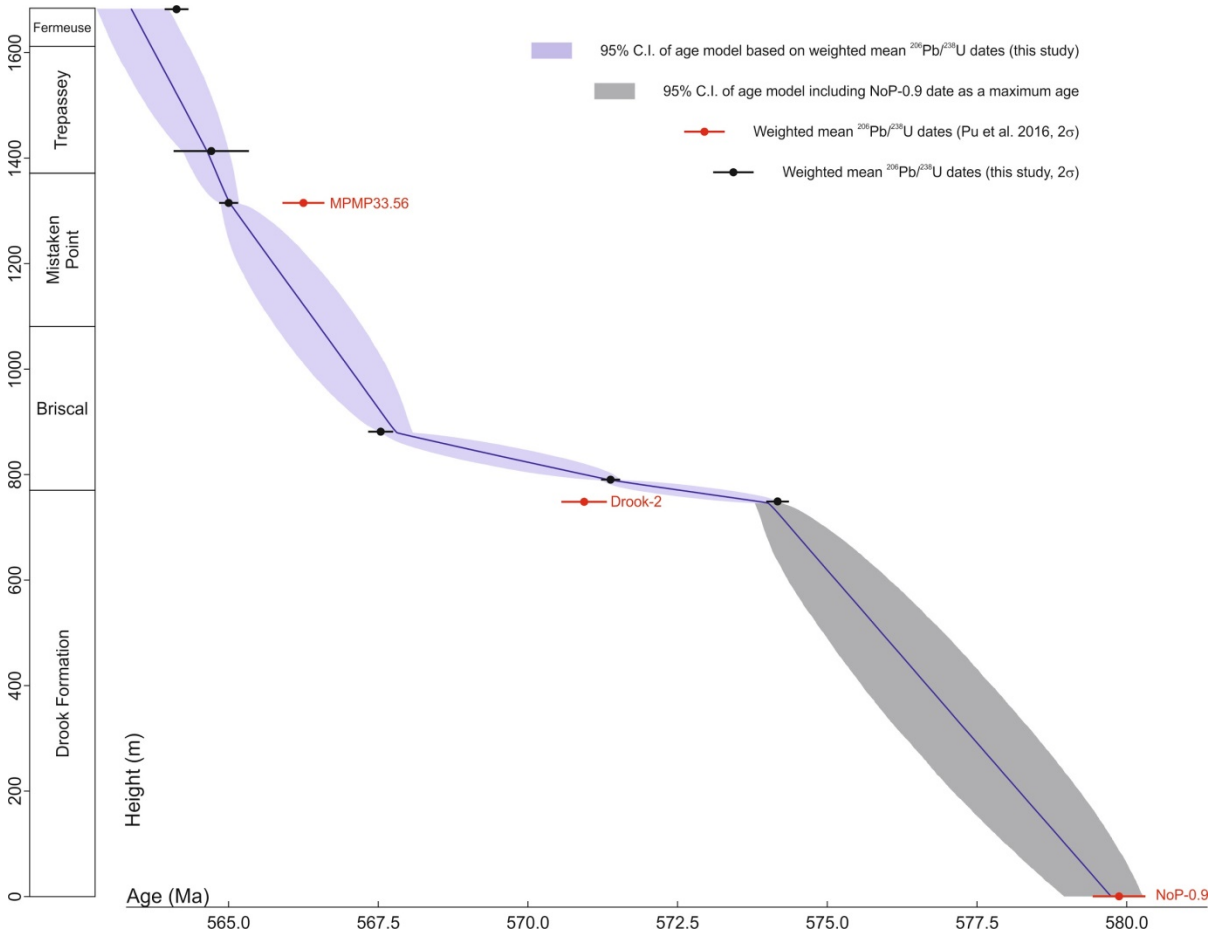

Figure S10. Extended age-depth model the Conception and St John's Groups using the approach outlined in the manuscript using dates from the Drook, Briscal and Mistaken Point, Trepassey and Fermeuse Formations (this study), combined with data from the base of the Drook Formation (NoP-0.9) from Pu et al. (2016). This age model combines dates from the measured section at MPER, importing the basal Drook Formation age from St. Mary's Bay (~70 km away) and as such the position of the NoP-0.9 date in the MPER section is not known. This age model assumes that the measured thickness of the Drook Formation, where the base of the Formation is not exposed, in the MPER is a minimum thickness and as such the NoP-0.9 date is treated as a maximum age constraint.

REFERENCES CITED

Condon, D.J., Schoene, B., McLean, N.M., Bowring, S.A., and Parrish, R.R., 2015, Metrology and traceability of U–Pb isotope dilution geochronology (EARTHTIME Tracer Calibration Part I): Geochimica et Cosmochimica Acta, v. 164, p. 464–480, https://doi.org/10.1016/j.gca.2015.05.026.

Hiess J. Condon D.J. McLean N. Noble S.R., 2012, 238U/235U systematics in terrestrial U-bearing minerals: Science , v. 335, p. 1610–1614, https://doi.org/10.1126/science.1215507.

Krogh T.E., 1973, A low contamination method for the hydrothermal decomposition of zircon and extraction of U and Pb for isotopic age determinations: Geochimica et Cosmochimica Acta , v. 37, p. 485–494, https://doi.org/10.1016/0016-7037(73)90213-5.

Mattinson, J. M., 2005, Zircon U-Pb chemical abrasion ("CA-TIMS") method: Combined annealing and multi-step partial dissolution analysis for improved precision and accuracy of zircon ages: Chemical Geology, v. 220, p. 47–66.

McLean, N.M., Bowring, J.F., and Bowring, S.A., 2011, An algorithm for U-Pb isotope dilution data reduction and uncertainty propagation: Geochemistry Geophysics Geosystems, v. 12, Q0AA18, https://doi.org/10.1029/2010GC003478.

McLean, N.M., Condon, D.J., Schoene, B., and Bowring, S.A., 2015, Evaluating uncertainties in the calibration of isotopic reference materials and multi-element isotopic tracers (EARTHTIME tracer calibration part II): Geochimica et Cosmochimica Acta , v. 164, p. 481–501

Pu, J.P., Bowring, S.A., Ramezani, J., Myrow, P., Raub, T.D., Landing, E., Mills, A., Hodgin, E., and Macdonald, F.A., 2016, Dodging snowballs: Geochronology of the Gaskiers glaciation and the first appearance of the Ediacaran biota: Geology, v. 44, p. 955–958, https://doi.org/10.1130/G38284.1.

SUPPLEMENTARY INFORMATION 4 (SI4): U-Pb Compositional and Isotopic Data

	Dates (Ma)								Composition					Isotopic Ratios							
Sample	206Pb/ 238U	±2σ	207Pb/ 235U b	±2σ	207Pb/ 206Pb	±2σ	Corr.		mass	Th/	Pb*	Pbc	Pb*/	206Pb/	208Pb/	206Pb/ 238U		207Pb/		207Pb/ 206Pb	
Fraction	<Th> a	abs		abs	<Th> a	abs	coef.	% disc c	U(pg)	U d	(pg) e	(pg) f	Pbc g	204Pb h	206Pb i	<Th> ia	±2σ %	235U i	±2σ %	<Th> ia	±2σ %
DRK-10																					
z12	**573.36**	**0.69**	**573.13**	**0.90**	**572.23**	**3.43**	**0.64**	**-0.16**	**114.1**	**1.65**	**14.4**	**0.17**	**86.7**	**4027.4**	**0.511**	**0.09302**	**0.126**	**0.7585**	**0.21**	**0.0592**	**0.15**
z2	**574.11**	**0.26**	**573.90**	**0.99**	**573.07**	**4.76**	**0.24**	**-0.14**	**224.0**	**1.36**	**26.6**	**0.59**	**45.2**	**2233.7**	**0.423**	**0.09314**	**0.047**	**0.7598**	**0.23**	**0.0592**	**0.22**
z7	**574.35**	**2.56**	**574.40**	**2.39**	**574.59**	**3.41**	**0.96**	**0.09**	**204.5**	**1.31**	**24.1**	**0.35**	**69.2**	**3445.5**	**0.408**	**0.09319**	**0.466**	**0.7607**	**0.55**	**0.0592**	**0.15**
z10	**574.43**	**0.32**	**574.23**	**1.01**	**573.43**	**4.39**	**0.57**	**-0.13**	**272.9**	**1.37**	**32.5**	**0.62**	**52.7**	**2598.8**	**0.425**	**0.09320**	**0.059**	**0.7604**	**0.23**	**0.0592**	**0.20**
z3	575.54	0.27	575.45	0.85	575.08	3.78	0.50	-0.04	180.1	1.41	21.7	0.34	63.4	3092.5	0.439	0.09339	0.049	0.7625	0.19	0.0592	0.17
z8	575.75	0.42	574.69	1.91	570.53	9.35	0.16	-0.87	231.5	1.42	28.0	1.15	24.2	1192.7	0.441	0.09342	0.076	0.7612	0.44	0.0591	0.43
z4	576.48	1.11	575.91	2.22	573.66	10.36	0.34	-0.46	110.4	1.77	14.3	0.54	26.4	1207.9	0.550	0.09355	0.201	0.7633	0.51	0.0592	0.48
z1	576.65	1.27	575.92	1.15	573.05	2.64	0.89	-0.58	231.4	1.41	27.9	0.29	95.0	4625.1	0.439	0.09358	0.231	0.7633	0.26	0.0592	0.12
z9	577.38	0.67	576.28	1.33	571.94	5.71	0.50	-0.90	147.8	1.24	17.2	0.46	37.8	1922.6	0.385	0.09370	0.122	0.7639	0.30	0.0592	0.26
DRK-1																					
z20A	**571.02**	**0.31**	**571.38**	**1.17**	**572.81**	**5.55**	**0.33**	**0.37**	**126.8**	**0.77**	**13.1**	**0.31**	**43.0**	**2426.0**	**0.240**	**0.09262**	**0.057**	**0.7554**	**0.27**	**0.0592**	**0.25**
z15	**571.12**	**0.78**	**568.33**	**3.62**	**557.15**	**17.57**	**0.27**	**-2.46**	**64.2**	**1.19**	**7.3**	**0.60**	**12.2**	**638.3**	**0.370**	**0.09264**	**0.143**	**0.7502**	**0.83**	**0.0588**	**0.80**
z19	**571.31**	**0.37**	**572.27**	**0.64**	**576.07**	**2.48**	**0.65**	**0.89**	**910.1**	**0.69**	**92.5**	**0.70**	**132.1**	**7566.4**	**0.215**	**0.09267**	**0.068**	**0.7570**	**0.15**	**0.0593**	**0.11**
z13	**571.34**	**0.35**	**570.32**	**0.96**	**566.24**	**4.52**	**0.32**	**-0.84**	**299.3**	**0.74**	**30.8**	**0.62**	**49.5**	**2808.6**	**0.231**	**0.09268**	**0.064**	**0.7536**	**0.22**	**0.0590**	**0.21**
z7	**571.49**	**1.20**	**574.48**	**6.91**	**586.32**	**33.56**	**0.20**	**2.60**	**189.0**	**0.55**	**18.5**	**3.69**	**5.0**	**315.1**	**0.170**	**0.09270**	**0.220**	**0.7608**	**1.57**	**0.0596**	**1.55**
z8	**571.76**	**0.58**	**572.48**	**2.00**	**575.37**	**9.36**	**0.35**	**0.67**	**125.9**	**1.34**	**14.8**	**0.63**	**23.6**	**1180.9**	**0.415**	**0.09275**	**0.105**	**0.7574**	**0.46**	**0.0593**	**0.43**
z1	**571.76**	**0.35**	**571.74**	**0.71**	**571.66**	**2.91**	**0.60**	**0.05**	**770.2**	**0.68**	**78.1**	**1.04**	**74.8**	**4301.9**	**0.212**	**0.09275**	**0.063**	**0.7561**	**0.16**	**0.0592**	**0.13**
z11	**571.98**	**1.11**	**573.53**	**6.15**	**579.64**	**29.82**	**0.22**	**1.38**	**65.1**	**0.99**	**7.1**	**1.11**	**6.4**	**359.6**	**0.308**	**0.09278**	**0.202**	**0.7592**	**1.40**	**0.0594**	**1.37**
z14	572.03	0.34	564.63	2.52	534.95	14.53	-1.32	-6.87	122.7	1.04	13.5	0.68	19.9	1066.7	0.323	0.09279	0.063	0.7438	0.58	0.0582	0.66
z18	572.04	0.23	572.06	0.65	572.12	2.86	0.51	0.07	157.6	0.88	16.8	0.21	79.5	4357.7	0.273	0.09279	0.042	0.7566	0.15	0.0592	0.13
z18A	572.34	0.51	573.85	2.66	579.81	12.96	0.18	1.34	45.2	0.98	4.9	0.29	17.0	924.3	0.303	0.09285	0.093	0.7597	0.61	0.0594	0.60
z4	572.44	1.14	572.26	4.50	571.52	19.29	0.74	-0.09	459.4	0.63	46.1	2.25	20.4	1202.8	0.197	0.09286	0.208	0.7570	1.03	0.0591	0.89
z16	572.60	0.43	572.25	1.54	570.87	7.41	0.26	-0.23	149.0	0.55	14.7	0.56	26.1	1560.6	0.172	0.09289	0.079	0.7569	0.35	0.0591	0.34
z17	572.64	0.40	572.13	1.67	570.10	7.82	0.41	-0.38	108.9	0.86	11.6	0.47	24.8	1377.8	0.267	0.09290	0.073	0.7567	0.38	0.0591	0.36
z3	574.11	0.54	573.75	1.97	572.34	9.25	0.36	-0.25	195.6	0.73	20.1	0.96	20.9	1201.3	0.226	0.09314	0.099	0.7596	0.45	0.0592	0.42
z5	575.03	0.83	574.69	2.35	573.32	10.74	0.41	-0.26	167.9	1.45	20.4	0.99	20.5	1006.4	0.449	0.09330	0.150	0.7612	0.54	0.0592	0.49
z9	577.03	0.61	577.91	1.04	581.37	4.16	0.60	0.81	551.6	0.62	55.6	1.03	53.9	3153.8	0.191	0.09364	0.110	0.7668	0.24	0.0594	0.19
z2	579.80	1.56	581.09	9.42	586.12	45.40	0.20	1.12	38.0	1.44	4.6	1.01	4.6	240.6	0.446	0.09411	0.281	0.7723	2.13	0.0595	2.09
z6	580.06	0.80	578.04	2.39	570.09	11.03	0.37	-1.70	93.0	1.23	10.9	0.52	20.8	1067.7	0.383	0.09415	0.145	0.7670	0.54	0.0591	0.51
BRS-1																					
z3	566.33	0.29	566.34	0.55	566.39	2.45	0.48	0.07	337.3	0.94	36.0	0.19	190.5	10279.9	0.292	0.09183	0.053	0.7468	0.13	0.0590	0.11
z6	**567.03**	**0.77**	**567.13**	**3.96**	**567.55**	**19.42**	**0.21**	**0.14**	**86.6**	**1.39**	**10.2**	**0.92**	**11.1**	**559.8**	**0.432**	**0.09194**	**0.141**	**0.7481**	**0.91**	**0.0590**	**0.89**
z5	**567.33**	**0.55**	**568.37**	**2.59**	**572.53**	**12.67**	**0.20**	**0.96**	**71.4**	**0.98**	**7.7**	**0.48**	**16.0**	**870.9**	**0.304**	**0.09200**	**0.101**	**0.7502**	**0.59**	**0.0592**	**0.58**
z9	**567.51**	**0.34**	**567.20**	**0.83**	**565.94**	**3.92**	**0.34**	**-0.21**	**221.0**	**0.77**	**22.8**	**0.43**	**53.3**	**3002.9**	**0.241**	**0.09203**	**0.062**	**0.7482**	**0.19**	**0.0590**	**0.18**
z4	**567.96**	**0.50**	**566.74**	**2.41**	**561.85**	**11.81**	**0.22**	**-1.02**	**54.4**	**0.84**	**5.7**	**0.32**	**18.0**	**1008.7**	**0.260**	**0.09210**	**0.093**	**0.7474**	**0.55**	**0.0589**	**0.54**
z2	**568.02**	**0.49**	**568.10**	**1.15**	**568.39**	**5.32**	**0.38**	**0.13**	**137.9**	**0.83**	**14.4**	**0.39**	**36.6**	**2040.0**	**0.258**	**0.09211**	**0.090**	**0.7498**	**0.26**	**0.0591**	**0.24**
z8	569.60	0.88	571.65	2.96	579.78	14.16	0.27	1.81	81.8	0.88	8.7	0.65	13.4	749.1	0.275	0.09238	0.162	0.7559	0.68	0.0594	0.65
z7	570.63	0.54	572.39	2.85	579.39	13.89	0.19	1.57	61.6	0.88	6.5	0.48	13.7	764.3	0.272	0.09256	0.098	0.7572	0.65	0.0594	0.64
MP-14																					
z16	563.81	0.62	564.38	1.29	566.67	5.24	0.64	0.57	78.7	0.63	7.8	0.20	38.1	2227.9	0.197	0.09140	0.115	0.7434	0.30	0.0590	0.24

z15	**564.74**	**0.50**	**565.76**	**1.26**	**569.85**	**5.58**	**0.52**	**0.96**	**91.7**	**0.65**	**9.1**	**0.20**	**45.2**	**2630.1**	**0.202**	**0.09156**	**0.093**	**0.7458**	**0.29**	**0.0591**	**0.25**
z2	**564.95**	**0.21**	**565.31**	**0.74**	**566.75**	**3.66**	**0.19**	**0.38**	**144.4**	**0.88**	**15.2**	**0.26**	**59.4**	**3256.7**	**0.274**	**0.09159**	**0.039**	**0.7450**	**0.17**	**0.0590**	**0.16**
z12	**565.10**	**0.37**	**565.50**	**1.60**	**567.11**	**7.54**	**0.41**	**0.42**	**274.7**	**0.54**	**26.6**	**1.14**	**23.3**	**1399.5**	**0.169**	**0.09162**	**0.068**	**0.7453**	**0.37**	**0.0590**	**0.34**
z4	**565.37**	**0.53**	**564.39**	**2.98**	**560.43**	**14.60**	**0.25**	**-0.81**	**174.3**	**0.71**	**17.6**	**1.10**	**16.0**	**930.4**	**0.220**	**0.09166**	**0.097**	**0.7434**	**0.69**	**0.0588**	**0.67**
z1	566.05	0.31	566.21	0.73	566.87	3.40	0.37	0.22	198.6	0.58	19.4	0.30	64.7	3823.3	0.179	0.09178	0.057	0.7465	0.17	0.0590	0.15
z14	566.18	0.33	566.91	1.59	569.84	7.82	0.19	0.72	117.5	0.49	11.2	0.50	22.6	1378.2	0.151	0.09180	0.061	0.7477	0.37	0.0591	0.36
z13	566.26	0.34	566.42	0.90	567.06	3.92	0.56	0.21	154.8	0.59	15.2	0.28	54.2	3195.0	0.184	0.09181	0.063	0.7469	0.21	0.0590	0.18
z9	566.96	0.42	566.78	1.88	566.07	9.12	0.27	-0.09	189.5	0.68	19.0	0.94	20.3	1178.8	0.212	0.09193	0.078	0.7475	0.43	0.0590	0.42
z5	567.19	1.01	566.50	1.40	563.74	4.79	0.75	-0.54	169.1	0.55	16.5	0.21	77.8	4619.7	0.172	0.09197	0.186	0.7470	0.32	0.0589	0.22
z6	567.48	0.32	567.24	0.67	566.26	3.21	0.31	-0.15	816.3	0.78	84.2	1.14	73.7	4135.5	0.243	0.09202	0.058	0.7483	0.15	0.0590	0.14
LC-1																					
z6B	**564.68**	**1.23**	**565.22**	**1.62**	**567.40**	**6.44**	**0.61**	**0.55**	**918.5**	**0.55**	**88.9**	**3.30**	**27.0**	**1615.8**	**0.170**	**0.09155**	**0.228**	**0.7448**	**0.37**	**0.0590**	**0.29**
z10	**564.72**	**0.73**	**564.69**	**0.72**	**564.57**	**2.19**	**0.80**	**0.04**	**1805.2**	**0.62**	**178.0**	**0.92**	**193.2**	**11248.5**	**0.193**	**0.09155**	**0.136**	**0.7439**	**0.17**	**0.0590**	**0.10**
z6A	565.53	0.61	565.77	0.80	566.75	3.10	0.64	0.29	757.3	0.58	74.1	1.24	59.7	3524.7	0.180	0.09169	0.112	0.7458	0.19	0.0590	0.14
z8	565.92	0.31	565.73	0.42	564.99	1.56	0.68	-0.10	1279.2	0.66	127.7	0.62	207.0	11937.3	0.205	0.09176	0.057	0.7457	0.10	0.0590	0.06
z2	565.92	0.19	565.92	0.42	565.91	1.76	0.62	0.07	1058.8	0.58	103.7	0.92	112.1	6596.7	0.181	0.09176	0.035	0.7460	0.10	0.0590	0.07
z3	566.30	0.29	566.24	0.47	566.00	1.90	0.61	0.01	2229.1	0.65	222.1	1.81	122.6	7094.2	0.202	0.09182	0.054	0.7466	0.11	0.0590	0.08
z5	566.32	0.22	566.38	0.63	566.63	2.99	0.31	0.12	1286.9	0.61	126.8	2.05	61.9	3628.4	0.188	0.09183	0.040	0.7468	0.14	0.0590	0.13
z11	566.48	0.30	566.28	0.41	565.48	1.49	0.69	-0.11	1599.5	0.62	158.4	0.74	212.8	12376.7	0.194	0.09185	0.056	0.7467	0.09	0.0590	0.06
z7	566.64	0.33	566.39	0.39	565.37	1.47	0.66	-0.16	615.7	0.69	62.0	0.34	181.2	10368.5	0.215	0.09188	0.060	0.7468	0.09	0.0590	0.06
z12	567.24	0.43	566.93	0.56	565.66	2.19	0.62	-0.21	1228.8	0.56	119.8	1.25	95.6	5662.5	0.173	0.09198	0.078	0.7478	0.13	0.0590	0.10
z13	567.41	2.98	567.26	2.47	566.64	3.96	0.96	-0.07	2474.0	0.59	243.6	2.51	97.1	5700.1	0.185	0.09201	0.549	0.7483	0.57	0.0590	0.18
SH-2																					
z15	**563.67**	**0.43**	**563.51**	**0.22**	**562.84**	**1.74**	**0.32**	**-0.08**	**464.9**	**0.61**	**45.6**	**0.21**	**219.1**	**12786.4**	**0.190**	**0.09138**	**0.080**	**0.7419**	**0.05**	**0.0589**	**0.07**
z16	**563.95**	**0.70**	**563.64**	**0.84**	**562.40**	**3.12**	**0.68**	**-0.20**	**278.2**	**0.51**	**26.7**	**0.24**	**110.4**	**6614.3**	**0.160**	**0.09142**	**0.130**	**0.7421**	**0.19**	**0.0589**	**0.14**
z9	**564.03**	**0.63**	**564.02**	**0.72**	**563.95**	**2.56**	**0.71**	**0.06**	**496.4**	**0.55**	**48.0**	**0.38**	**125.3**	**7431.2**	**0.171**	**0.09144**	**0.116**	**0.7428**	**0.17**	**0.0589**	**0.11**
z14	**564.24**	**0.73**	**563.75**	**0.84**	**561.76**	**3.50**	**0.58**	**-0.37**	**495.3**	**0.55**	**48.0**	**0.61**	**78.8**	**4677.2**	**0.172**	**0.09147**	**0.135**	**0.7423**	**0.19**	**0.0589**	**0.16**
z19	**564.31**	**0.39**	**564.40**	**0.46**	**564.79**	**1.63**	**0.71**	**0.16**	**612.9**	**0.50**	**58.6**	**0.21**	**283.7**	**17022.7**	**0.155**	**0.09148**	**0.071**	**0.7434**	**0.11**	**0.0590**	**0.07**
z12	**564.39**	**0.40**	**564.32**	**0.63**	**564.03**	**2.66**	**0.56**	**0.01**	**226.0**	**0.48**	**21.5**	**0.23**	**92.6**	**5594.3**	**0.150**	**0.09150**	**0.074**	**0.7433**	**0.15**	**0.0589**	**0.12**
z3	564.66	0.22	564.68	0.42	564.72	1.64	0.69	0.08	652.5	0.54	63.0	0.43	146.9	8738.5	0.167	0.09154	0.040	0.7439	0.10	0.0590	0.07
z5	564.85	0.21	564.70	0.57	564.13	2.56	0.48	-0.05	813.0	0.44	76.5	1.04	73.5	4493.2	0.136	0.09158	0.039	0.7439	0.13	0.0589	0.11
z1	565.55	0.19	565.55	0.38	565.54	1.65	0.53	0.07	812.2	0.55	78.9	0.57	138.4	8199.2	0.172	0.09169	0.035	0.7454	0.09	0.0590	0.07
z2	568.16	0.56	567.65	0.68	565.58	2.50	0.68	-0.39	687.8	0.57	67.4	0.77	88.1	5205.2	0.178	0.09214	0.103	0.7490	0.16	0.0590	0.11
z7	569.01	0.68	568.15	0.71	564.74	2.23	0.78	-0.68	504.8	0.47	48.3	0.48	100.3	6079.4	0.146	0.09228	0.125	0.7499	0.16	0.0590	0.10

a Corrected for initial Th/U disequilibrium using radiogenic 208Pb and Th/U[magma] = 2.8 ± 1.0 (2σ).

b Isotopic dates calculated using λ238 = 1.55125E-10 (Jaffey et al. 1971) and λ235 = 9.8485E-10 (Jaffey et al. 1971).

c % discordance = 100 - (100 * (206Pb/238U date) / (207Pb/206Pb date))

d Th contents calculated from radiogenic 208Pb and 230Th-corrected 206Pb/238U date of the sample, assuming concordance between U-Pb Th-Pb systems.

e Total mass of radiogenic Pb.

f Total mass of common Pb.

g Ratio of radiogenic Pb (including 208Pb) to common Pb.

h Measured ratio corrected for fractionation and spike contribution only.

i Measured ratios corrected for fractionation, tracer and blank.

All common Pb assumed to be laboratory blank. Total procedural blank 0.05 ± 0.02 (2σ) pg for U.

Blank isotopic composition: $^{206}Pb/^{204}Pb$ = 18.10 ± 0.27, $^{207}Pb/^{204}Pb$ =15.55 ± 0.14, $^{208}Pb/^{204}Pb$ = 37.82 ± 0.41 (1σ).